International Refereed Journal of Engineering and Science (IRJES)
ISSN (Online) 2319-183X, (Print) 2319-1821
Volume 7, Issue 5 Ver. I (May 2018), PP. 18-29

A Novel Dc Voltage Detection Technique in Cascaded H-Bridge Multilevel Converter Based Photovoltaic System

Harsha Patle[1], Pranita Chavan[2]
[1]*Student, Department of Electrical Engg, YTIET, Karjat, Raigad, Maharashtra*
[2] *Asst. Professor, Department of Electrical Engg, Pillai college of engg, Panvel, Raigad, Maharasthra*
Corresponding Author: Harsha Patle

ABSTRACT:-In this paper a cascaded H-Bridge multilevel converter based Photovoltaic (PV) system with no voltage or current sensors at the dc-side is proposed. Removing the dc-side sensors simplifies the hardware, resulting in lower cost and higher reliability of the PV system. A novel dc voltage detection technique is established by estimating the capacitors' voltages from the output ac voltage of the inverter using single voltage sensor at the ac side of the converter. The scheme allows replacing all dc-side voltage sensors by a single voltage sensor at the ac-side of the converter. Furthermore, the dc current sensors, conventionally required for the maximum power tracking (MPPT), are also removed. Instead, the outputs from the capacitors' voltage control systems are utilized for the MPPT. The effectiveness of the proposed system with no voltage and current at dc side of the converter is demonstrated on a 2 kW single-phase 7-level CHB converter based PV system.The results are obtained from the MATLAB/ SIMULINK environment.
KEYWORDS:-Voltage Measurement, Voltage Control, Capacitors, Sensor System, Switches.

Date of Submission: 02-06-2018 Date of acceptance: 18-06-2018

I. INTRODUCTION

Now a days the renewable energy such as wind, solar, ocean, Biomass and geothermal powers are getting more attention with the increasing demand on energy, high oil prices and concern of environmental impacts increased. Among them Photovoltaic (PV) generation getting more importance due to absence of fuel cost, low maintenance, no noise, no moving parts and long life time. Multilevel inverters became more popular in the power conversion systems for high power and power quality demanding applications. Among different topologies of MLIs, Cascaded H-Bridge MLIs are more suitable converters for PV applications since each PV panel can act as a separate DC source for each CHB module.

In recent years, there has been an increasing interest in electrical power generation from renewable-energy sources, such as photovoltaic (PV) or wind-power systems. Among the different renewable-energy sources, solar energy has been one of the most dynamic research are as in the past decades, both for grid-connected and Stand-alone applications. The basic concept of PV cell is to gather solar energy from sun and transfer it for distribution as electrical power. However this collected solar energy requires conversion techniques to make them functional to the end users. Basically the output of the PV cell is DC form. For commercial purpose it needs to convert to AC form because most of the loads are AC loads.

Different topologies MLIs for the conversion from DC to AC are available such as Neutral point clamped MLI (NPC-MLI), Flying capacitor MLI (FC-MLI), Cascade H-Bridge MLI (CHB-MLI) and Asymmetrical Cascade H-Bridge Multilevel inverters. Among them CHB-MLIs are mostly used for PV applications because each cell of CHB-MLI requires separate DC sources which can be easily supplied by individual PV arrays and each H-Bridge cell will be available in a single module. The number of levels of the output wave form increased by cascading the number of H-Bridge cells.

Application of the cascaded H-bridge multilevel converters (CHB-MCs) in Photovoltaic (PV) systems has been studied in many technical papers [1]-[17]. Though, none of these studies have focused on shortening the system hardware by reducing the sensor count.

Reducing the sensor count is of great importance because having both the dc voltage and the dc current sensors for each H-bridge cell increases the system cost and complexity and also reduces its reliability. Furthermore, extending the capacity of an existing system by adding more cells becomes difficult due to additional wirings required for the sensors and a potentially limited number of I/O channels available on the central control board. Therefore, removing either or both the dc current or voltage sensors are valuable.

In a conventional PV system, both the dc current and voltage sensors are required by the Maximum Power Point Tracking (MPPT) algorithm. Several single voltage sensor PV systems were proposed in literature

[18]-[21]. In [18], paper presents a load-current-based maximum power point tracking (MPPT) digital controller with an adaptive step-size and adaptive-perturbation-frequency algorithm, the dc voltage sensor was removed and the MPPT was executed using the dc-dc converter's duty cycle and the dc current measurement. In [19], the MPPT was executed by only sensing the dc voltage. The change in the power delivered by the inverter was inferred from the control signals. Tracking the actual maximum power point of a PV array using only the voltage sensor was performed by connecting a capacitive load to it in [20], [21]. However, a specific type of converter was essential to implement the proposed technique. In summary, none of these studies were executed for a CHB-MC based PV system and in none of them were both the DC current and the dc voltage sensors removed.

In conventional CHB-MC based PV systems the dc current sensors are required by the MPPT module and the dc voltage sensors are required for the capacitors' voltages control system and the Pulse Width Modulation (PWM) generator. Hence, in higher level converters, many isolated dc sensors are required, which increases the system cost and complexity. The dc voltage sensors elimination in CHB-MCs was addressed in a few papers, but only for STATCOMs. The dc voltage sensors were replaced by a single sensor at the AC side of the CHB inverter-based STATCOM in [22]. The voltage measurement for each cell was performed at a specific moment of switching in which the output of all cells except one was zero. Therefore, the sampling frequency of capacitors' voltages measurement was low and varying, which is not desirable. This drawback was addressed in [23], where the sampling frequency was kept constant at twice the switching frequency. However, no experimental validation was provided. In [24], the capacitor voltage sensors were placed by an observer in the CHB based STATCOM. However, the slow dynamics of the observer makes this method not suitable to perform the PWM switching or fast voltage control.

In this paper, for the first time, a novel dc voltage detection technique CHBMC based PV system which does not require any dc current or dc voltage sensors is proposed.

II. PROPOSED SYSTEM

2.1 A CHB-MC Based PV control system

The CHB-MC allows controlling the individual capacitors' voltages independently; the PV modules can be connected directly to the dc-links, thus removing need for the dc–dc converters, as shown in Fig.1.

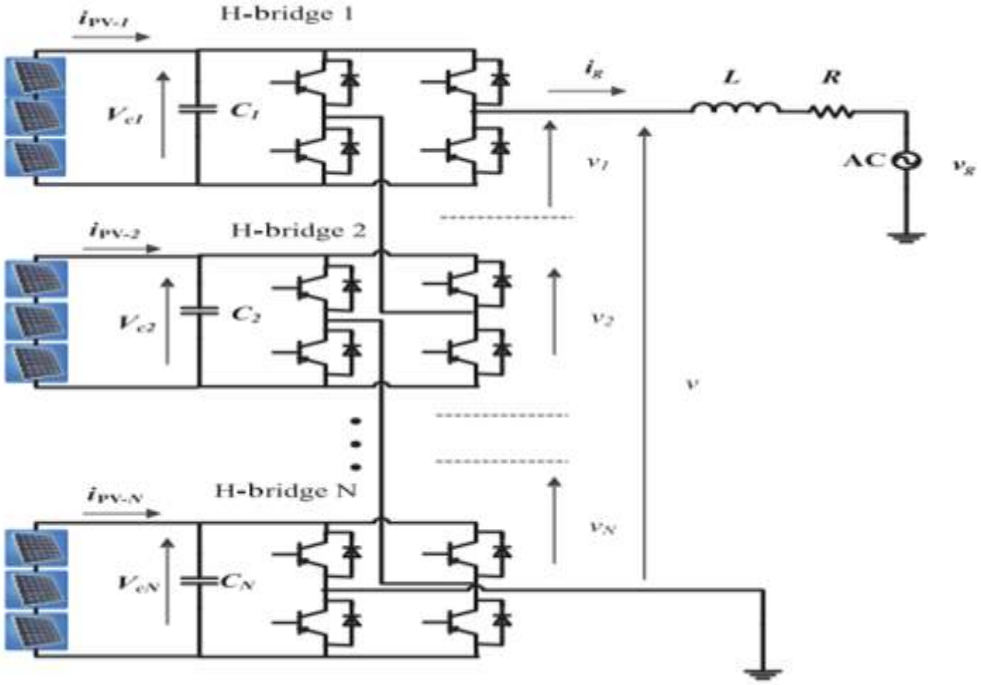

Fig.1: CHB-MC PV system

Since the output voltage of the PV modules can vary in a wide range due to partial shading, the PV modules are conventionally connected to a fixed dc link voltage of the inverter via a dc-dc converter. However, by presenting the DC-DC converter the overall efficiency of this configuration is reduced by 4-10% [25] and the cost and complexity of the system is increased. However, since the CHB-MC allows controlling the individual capacitors voltages individually, the PV modules can be connected directly to the dc links thus removing need for the dc-dc converters as shown in Fig. 1.Conventional control systems for this configuration require N H-

bridges, N voltage sensors, and N current sensors at the dc-side. In this paper, a dc-side sensor less control system for the configuration in Fig. 1 is proposed. The main advantage of the proposed control system, as compared to the conventional ones, is that all dc-side current and voltage sensors are removed, which considerably reduces the system's complication and cost. In the proposed control system, only one voltage sensor is required to measure the voltage at the ac-side of the CHB-MC. In addition, one voltage sensor is required to measure the grid voltage and one current sensor is required to measure the grid current.

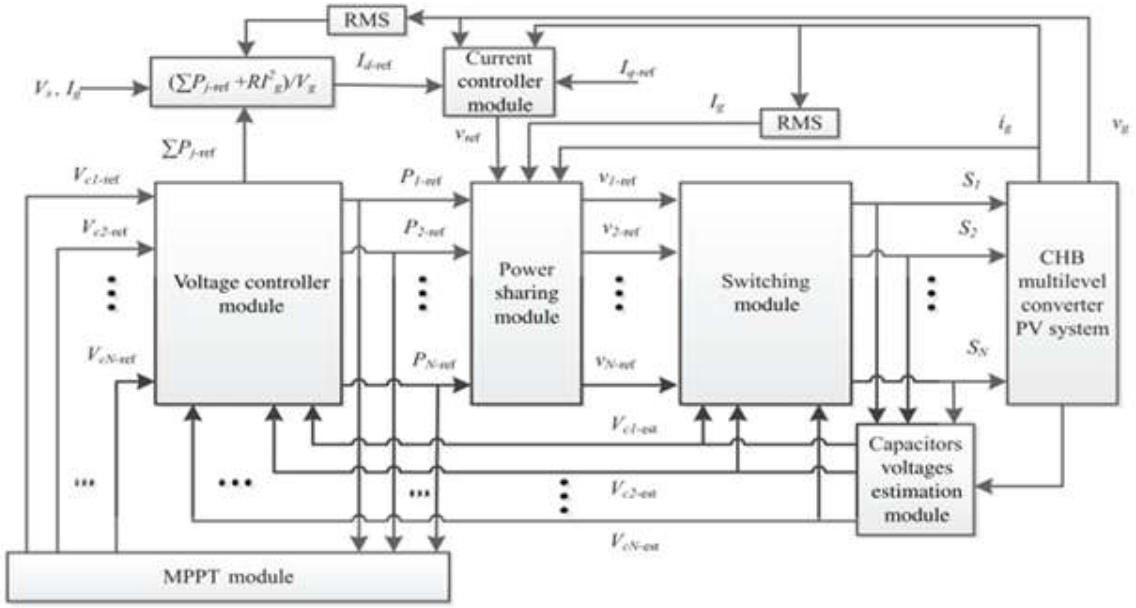

Fig.2: Block diagram of the dc voltage detection technique in CHB multilevel converter based photovoltaic system

Block diagram of the proposed control system is shown in Fig. 2. The ac output voltage *v* measured at the ac-side of the CHB-MC is used to estimate the capacitors' voltages in the Capacitors' Voltages Estimation Module (CVEM). The estimated capacitors voltages are then used (i) in the voltage controller module as feedback signals, (ii) in the switching module for feed forward compensation of the low order harmonic ripples and (iii) in the MPPT module to estimate the average PV modules power in order to track the optimal operating point. The measured grid voltage *vg*, and the grid current *ig* are used by the current controller module. *ig* is also used by the power sharing module to generate the voltage reference signals for the switching module. In the following sections, design and operation of each module is explained in detail.

2.2 Capacitors' voltages estimation module

The capacitors voltages are estimated using a single voltage sensor that measures the ac output voltage v at the ac-side of the CHB-MC. This allows removing all dc-side voltage measurement sensors.

The measured ac output voltage v, is sampled after each switching transition. Therefore, the voltage sampling frequency for each bridge is twice the switching frequency. The ac output voltage *v* in an (*N* + 1)-level CHB-MC is given by,

$$v = \sum_{j=1}^{N} S_j V_{c-j} - DV_{\text{diode}} - MV_{\text{switch}} \tag{1}$$

Where *Sj* = (0, +1, −1) is the switching function of the *j*th H-bridge, and *V*diode and *V*switch are the forward voltage drops across the conducting diode and switch, respectively. *D* and *M* represent the number of conducting diodes and switches, respectively, which can be calculated as [23]

Then, the capacitor voltage *Vc-j* of the *j*th switched bridge can be determined from the measured ac output voltage *v* before and after each switching transition as [23]

$$V_{c-j} = |v' - v''| \tag{2}$$

Where *v'* is the ac output voltage measured before and v'' after the switching transition

2.3 Voltage Controller module and MPPT module

The MPPT module and the Voltage Controller module are shown in Figs.3 and 4.

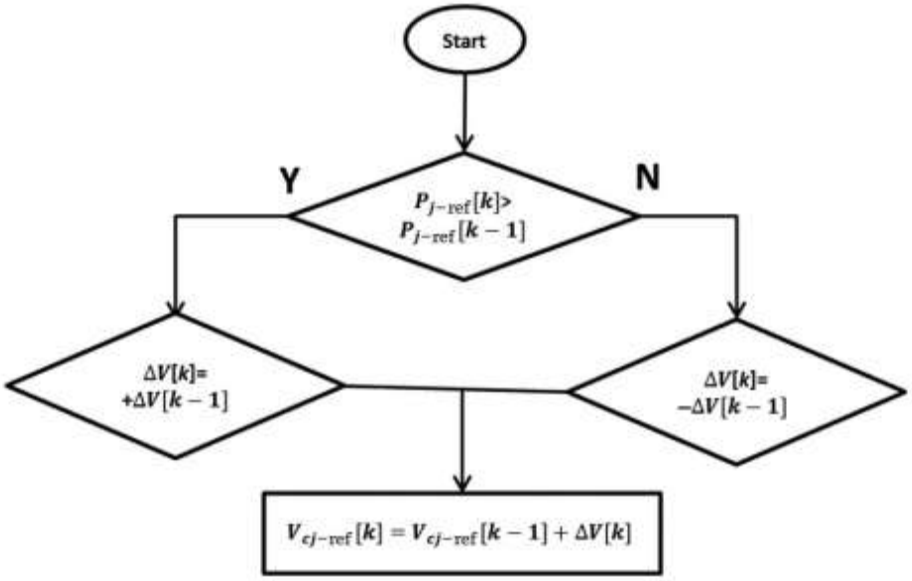

Fig.3: MPPT module (P&O algorithm)

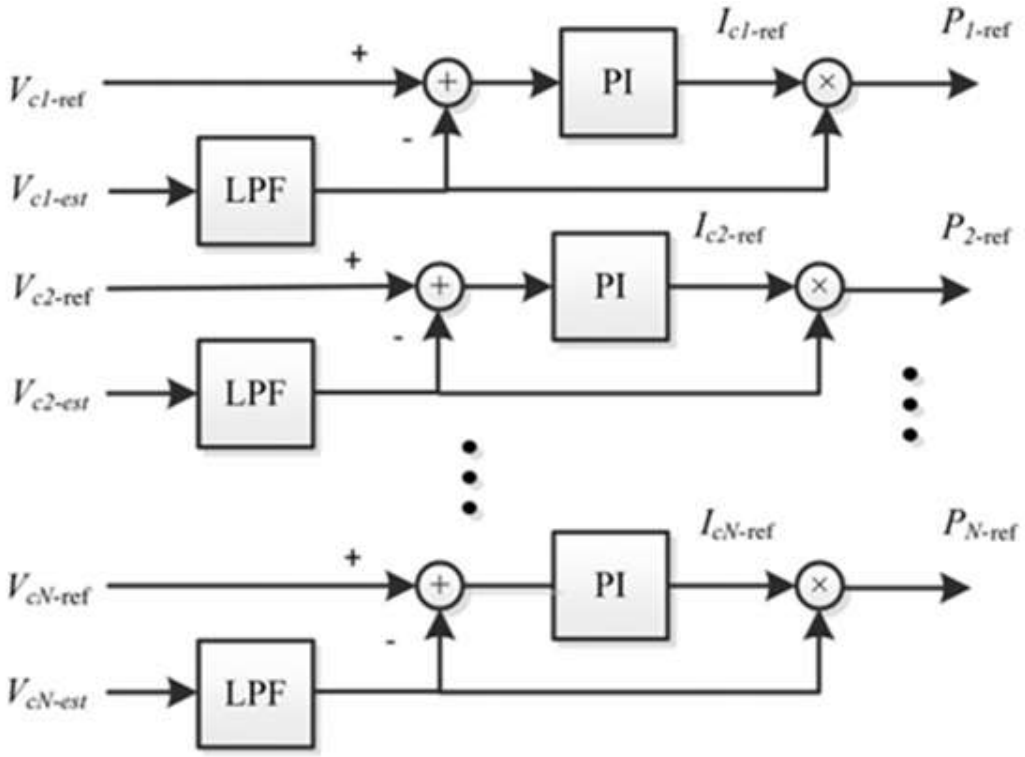

Fig.4:Voltage controller module

The voltage controller module consists of the proportional integral (PI) voltage controllers, which control each capacitor's voltage toward the reference values determined by the Perturb and Observe (P&O) algorithm implemented in the MPPT module.

2.4 Current controller module

Block diagram of the current controller module is shown in Fig.5.

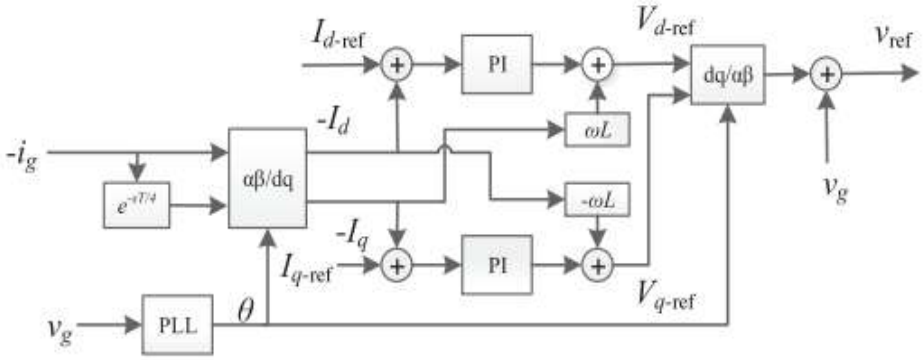

Fig.5: Current controller module

The current controller module controls the grid current in the *d*−*q* reference frame. As the system is single phase, the required quadrature signal of the grid current is generated by a quarter of a period delay function.

The grid current is governed by the following equation, which is obtained by applying Kirchhoff's voltage law to the ac side,

$$\sum_{j=1}^{N} v_j - v_g - Ri_g - L\frac{di_g}{dt} = 0, \quad j = 1, \ldots, N \tag{3}$$

where *vj* is the output voltage generated by the *j*th H-bridge, *L* represents the inductance of the filtering inductor, and *R* is its series resistance. *vg* and *ig* are the grid voltage and current, respectively.

The active-power reference current *Id*- r e f is calculated as,

$$I_{d\text{-ref}} = \left(\sum_{j=1}^{N} P_{j\text{-ref}} + RI_g^2 \right) / V_g \tag{4}$$

where *Ig* and *Vg* are the rms values of the grid current and voltage, respectively. The reactive power reference current *Iq*-ref is set to zero.

2.5 Power sharing module

This module is used to distribute the reference voltage *v*ref generated by the current controller between the H-bridges based on the reference powers *Pj*− ref from the voltage controller module. The module initially distributes the reference voltage among the H-Bridges equally. The active power that each H-bridge draws is calculated as,

$$P_m = \frac{\sum_{j=1}^{N} P_{j\text{-ref}}}{N}. \tag{5}$$

To regulate the active power drawn by the *j*th H-bridge to its reference value *Pj*− r e f, the module adjusts the reference voltage of the *j*th H-bridge *vj*− ref as,

$$v_{j\text{-ref}} = \frac{v_{\text{ref}}}{N} + \frac{P_{j\text{-ref}} - P_m}{I_g}\frac{i_g}{I_g}, \quad j = 1, \ldots, N. \tag{6}$$

2.6 Switching module

In the switching module, the estimated capacitors' voltages ripples are used for feed forward modification of the reference ac voltage signals. As a result, variations in the capacitors' voltages have minimal effect on the inverter ac voltages and current.

The phase-shifted (PS)-PWM technique is utilized to generate the switching signals for each H-bridge. Using the PS-PWM switching technique, the switching frequency of each module remains constant, which in theory results in sampling of the estimated capacitor' voltages at twice the switching frequency of each H-bridge. However, in practice, measurement of the output voltage at narrow pulses is difficult, less accurate, and requires fast analog-to-digital converter (ADC) modules. This issue can be resolved either by ignoring the narrow pulses in the CVEM or by removing/limiting the width of the narrow pulses in the switching module. In this paper, the first approach is used as modifying the generated output voltage would adversely affect the

current total harmonic distortion (THD) and increase the PWM module implementation complexity. Since the occurrence of pulses that are narrower than a minimal pulse width is infrequent, ignoring these pulses does not have any significant effect on the operation of the control system.

III. SIMULATION & RESULTS

A PV array connected to the grid through a 7-level CHB converter is used to simulate the operation of the proposed system. The PV array is composed of four subarrays and each subarray has two series connected REC220AE-US PV modules. The model of the REC220AEUS PV module and its parameters can be found in [29] and [30]. Each subarray feeds each H-bridge. The parameters of the simulated system are given in Table I.

Table I PARAMETERS OF THE SIMULATED SYSTEM

Symbol	Quantity	Value
$V_{g\text{-rms}}$	Grid voltage rms value	110 V
C	H-bridge dc capacitance	3.3×10^{-3} F
L	Filter inductance	2 mH
f_s	Switching frequency (per H-bridge)	1600 Hz
f_g	Grid frequency	50 Hz
S	Converter nominal power	1.8 kVAr
R	Filter inductor series resistance	0.2 Ω
f_v	Bandwidth of the voltage controller	10 Hz
f_i	Bandwidth of the current controller	200 Hz
f_m	MPPT update frequency	1 Hz
N	Number of H-bridges	4

The objective of the simulations presented in this section is to demonstrate that operation of the proposed dc-side sensorless control system is comparable to a conventional system with one dc voltage and one dc current sensor per H-bridge.

3.1 Simulation Models

The simulation model of the proposed dc-side sensorless control system and conventional system with one dc voltage and one dc current is developed using MATLAB as shown in figures below

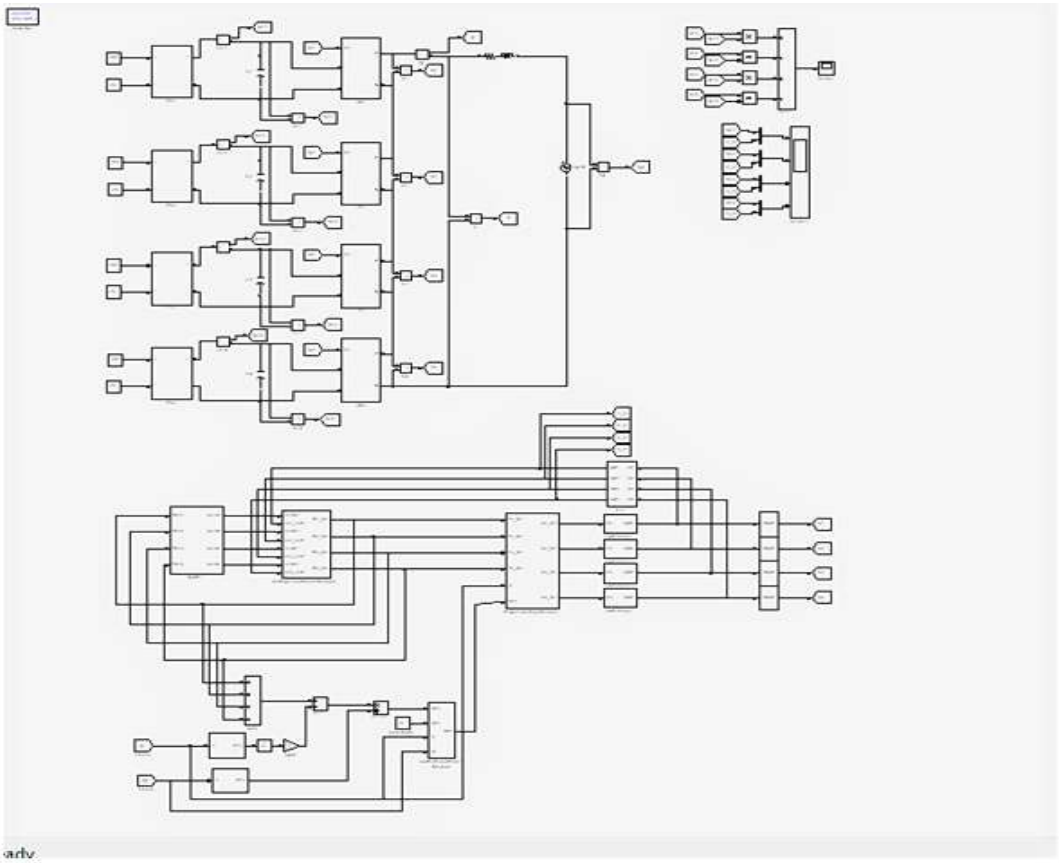

Fig. 6: Simulink model of the proposed DC-side sensorless control system

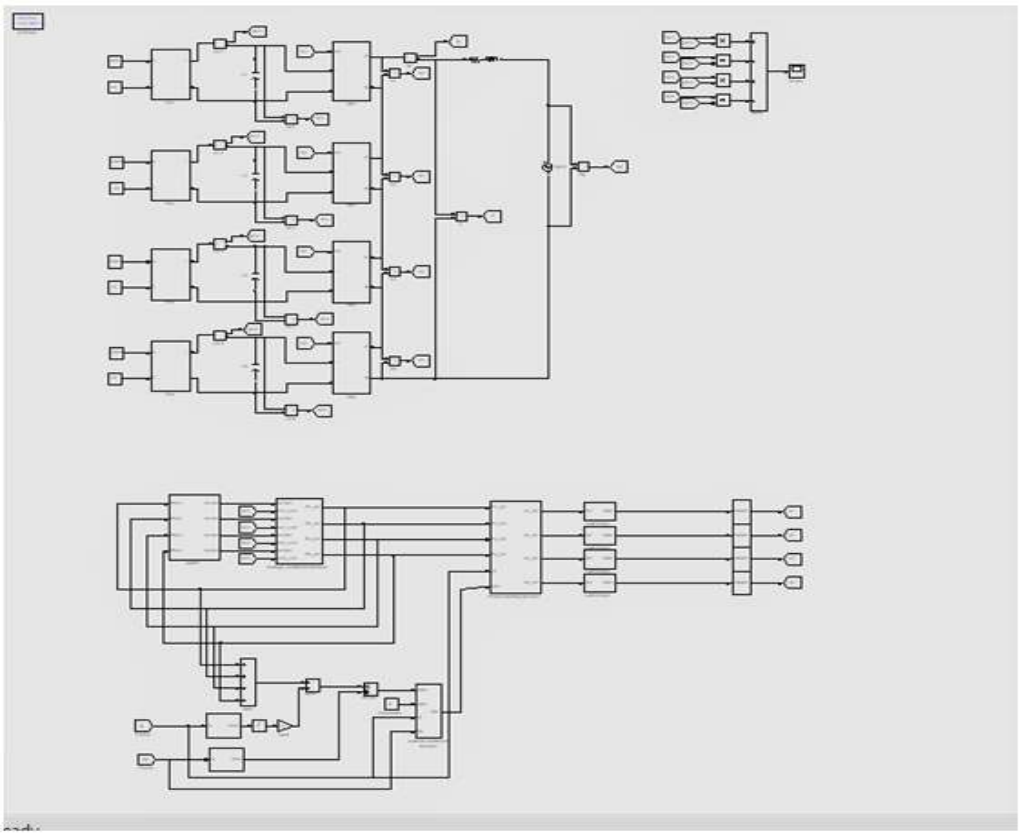

Fig.7: Simulink model of the conventional system

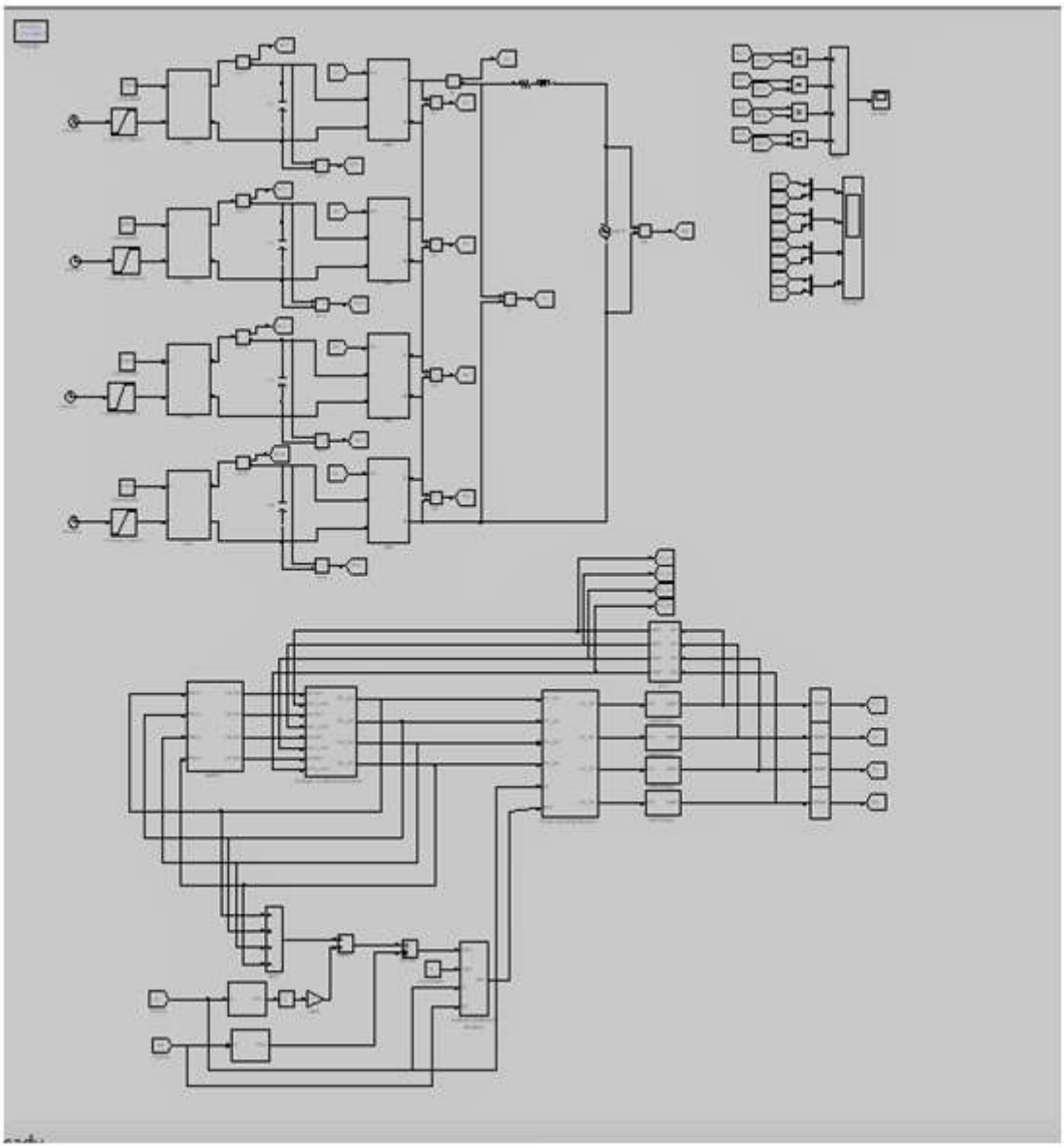

Fig.8: Simulink model of operation of CVEM

Operation of the CVEM is demonstrated in Fig.8. Initially, all capacitors' voltages are fixed to 55 V. Then, at time t = 1 s, the reference capacitor voltages of the H-bridges 1 and 2 are changed to 65 and 50 V, respectively. As it can be observed from the results, the CVEM is able to follow the actual voltages closely even during the transients.

3.2 Results

The results of the extracted power for both the conventional and proposed systems for four different cases are discussed as below

Case I

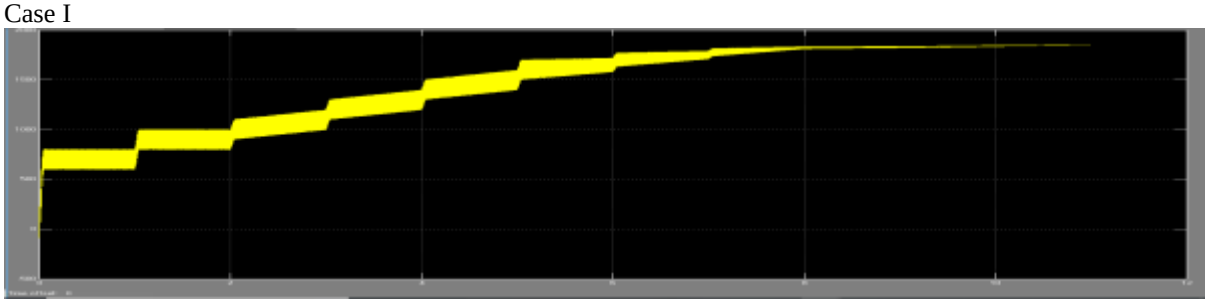

Case II

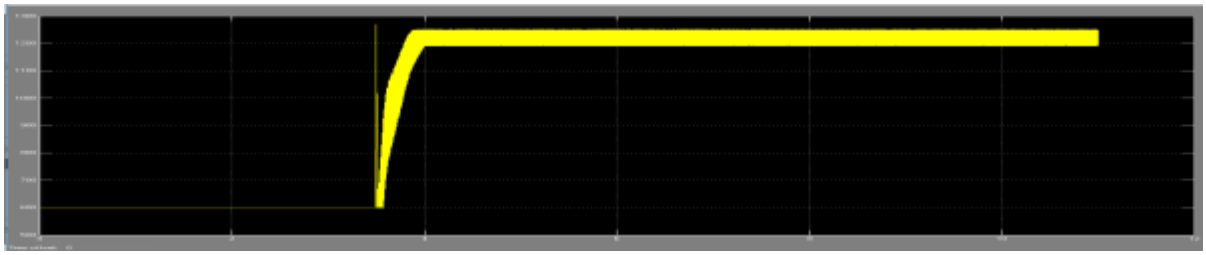

Case III

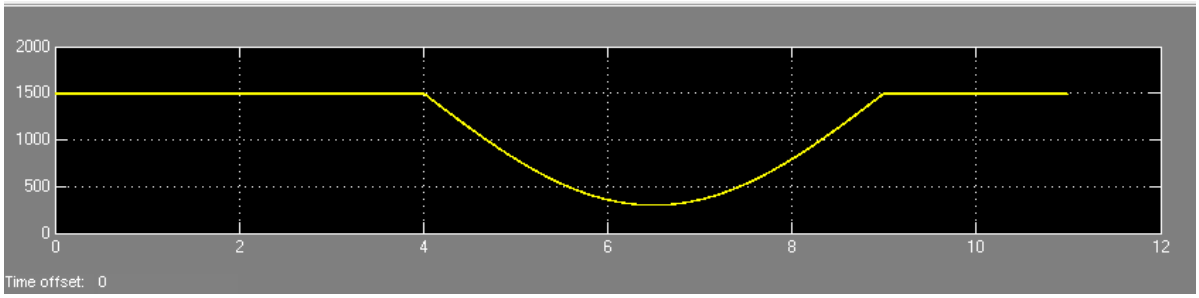

Case IV

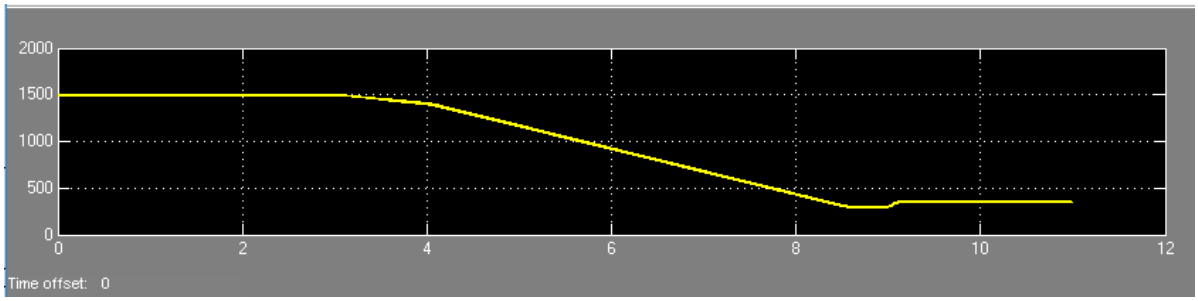

Fig.9(a):Output power of the proposed PV system. Case I: Startup test, Case II: Step radiation change from 400 to 800 W/m^2 at t=3.5 s, Case III: Gradual irradiance change, Case IV: Gradual temperature change.

Case I

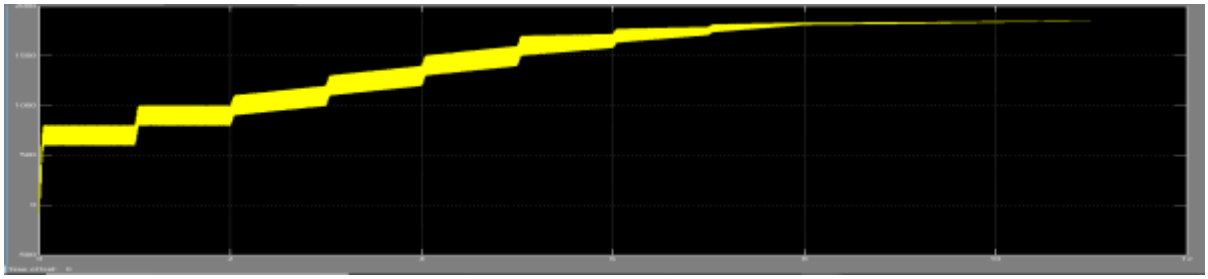

Case II

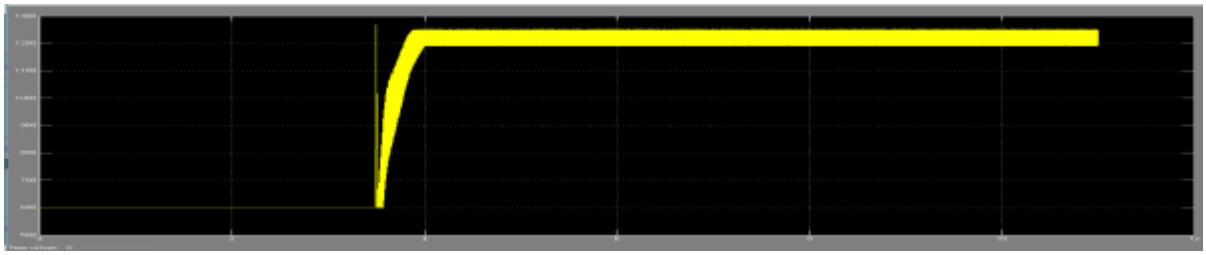

Case III

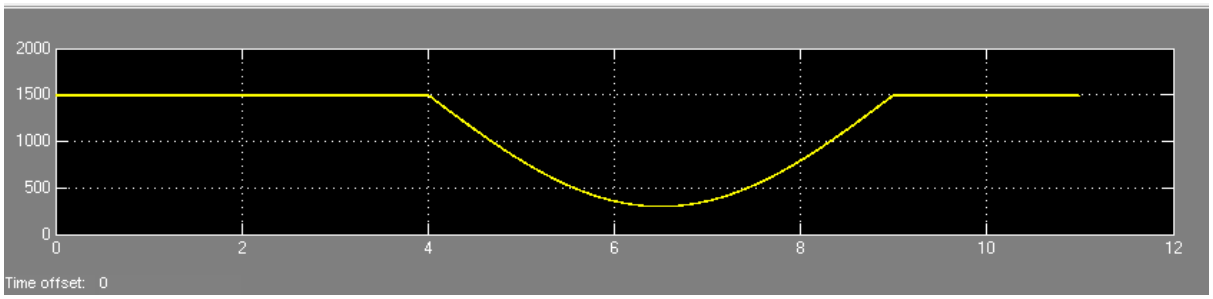

Case IV

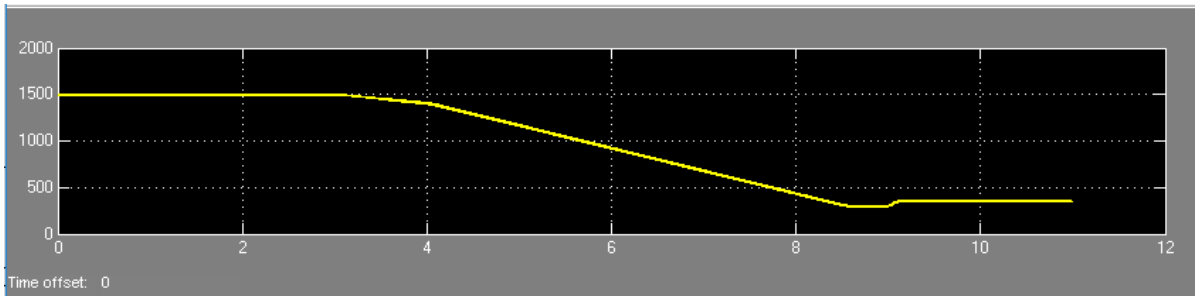

Fig.9(b):Output power of the conventional system with one dc voltage and one dc current sensor per H-bridge. Case I: Startup test, Case II: Step radiation change from 400 to 800 W/m^2 at t=3.5 s, Case III: Gradual irradiance change, Case IV: Gradual temperature change.

H-Bridge 1

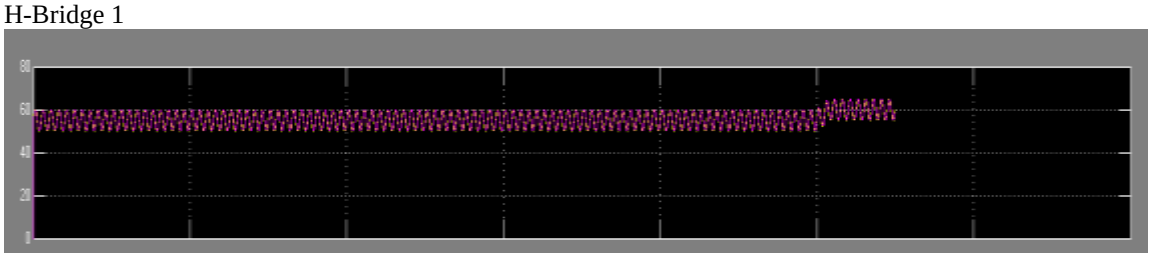

H-Bridge 2

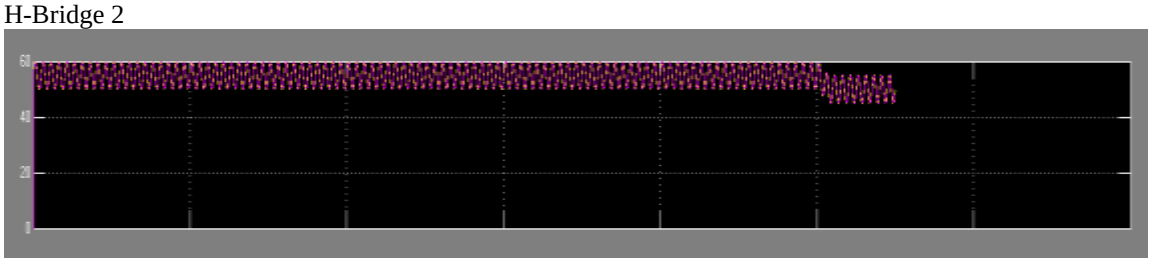

H-Bridge 3

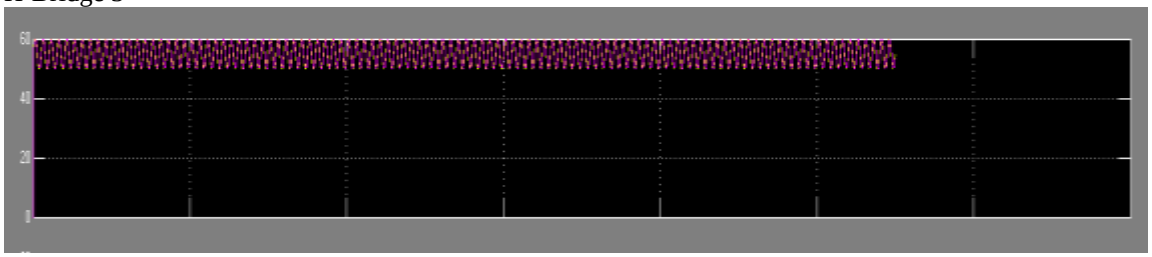

H-Bridge 4

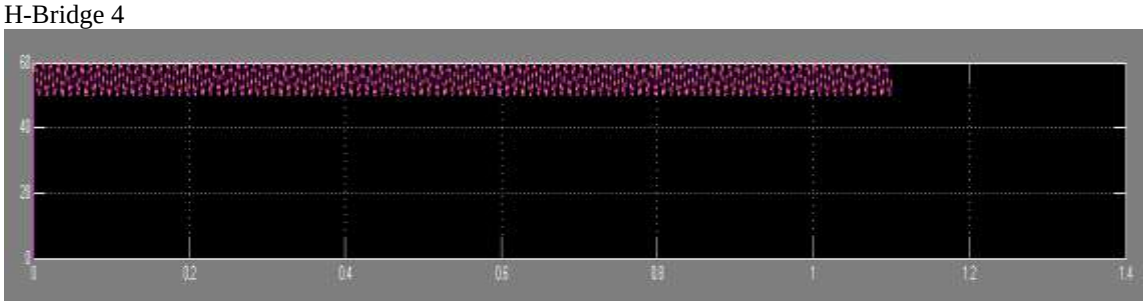

Fig.10: Comparison of the estimated and measured capacitors' voltages.

As it can be concluded in Fig.9, the performance of the proposed PV system closely matches the conventional one in all of the conducted simulation case studies. This demonstrates that the outer control loops of the control system that operate at low frequency (voltage control loop and the MPPT) are unaffected as the CVEM is able to update the capacitors voltages with much faster frequency.

Operation of the CVEM is demonstrated in Fig.10. Initially, all capacitors' voltages are fixed to 55 V. Then, at time t = 1 s, the reference capacitor voltages of the H-bridges 1 and 2 are changed to 65 and 50 V, respectively. As it can be observed from the results, the CVEM is able to follow the actual voltages closely even during the transients.

IV. CONCLUSION

A dc voltage detection technique in CHB MC based PV system has been proposed and experimentally verified. The experimental tests on a 7-level CHB MC based PV system showed that the performance of the proposed system was comparable with a conventional system that employed all dc-side sensors. The main benefits of removing the dc-side sensors are reduced cost, simpler hardware, and increased reliability of the PV system. The operation of the proposed control system under the switching devices failure has not been addressed in this work and needs to be studied in detail in the future to improve the reliability of the system.

REFERENCES

[1]. O. Alonso, P. Sanchis, E. Gubia, and L. Marroyo, "Cascaded H-bridge multilevel converter for grid connected photovoltaic generators with independent maximum power point tracking of each solar array," in *Proc .IEEE PESC*, 2003,vol.2,pp. 731–735C.

[2]. E. Villanueva, P. Correa, J. Rodriguez, and M. Pacas, "Control of a single-phase cascaded H-bridge multilevel inverter for grid-connected photovoltaic systems,"*IEEE Trans.Ind. Electron*., vol. 56, no. 11, pp. 4399–4406, Nov. 2009.

[3]. S. Kouro, W. Bin, A. Moya, E. Villanueva, P. Correa, and J. Rodriguez, "Control of a cascaded H-bridge multilevel converter for grid connection of photovoltaic systems," *in Proc. 35th Annu. Conf. IEEE Ind. Electon. (IECON)*, 2009, pp. 3976–3982.

[4]. C. Cecati, F. Ciancetta, and P. Siano, "A multilevel inverter for photovoltaic systems with fuzzy logic control," *IEEE Trans. Ind. Electron*., vol. 57, no. 12, pp. 4115–4125, Dec. 2010.

[5]. J. J. Negroni, D. Biel, F. Guinjoan, and C. Meza, "Energy-balance and sliding mode control strategies of a cascade H-bridge multilevel converter for grid-connected PV systems," in *Proc. IEEE Int. Conf. Ind. Technol. (ICIT)*, 2010, pp. 1155–1160.

[6]. M. Chithra and S. G. B. Dasan, "Analysis of cascaded H bridge multilevel inverters with photovoltaic arrays," *in Proc. Int. Conf. Emerg. Trends Elect. Comput. Technol. (ICETECT*), 2011, pp. 442–447.

[7]. S. Rivera, S. Kouro, B. Wu, J. I. Leon, J. Rodriguez, and L. G. Franquelo,"Cascaded H-bridge multilevel converter multistring topology for large scale photovoltaic systems," in *Proc. IEEE Int. Symp. Ind. Electron. (ISIE)*, 2011, pp. 1837–1844.

[8]. S. Rivera, W. Bin, S. Kouro, W. Hong, and Z. Donglai, "Cascaded H-bridge multilevel converter topology and three-phase balance control for large scale photovoltaic systems," in *Proc. 3rd IEEE Int. Symp. Power Electron. Distrib. Gener. Syst. (PEDG*), 2012, pp. 690–697.

[9]. J. Chavarria, D. Biel, F. Guinjoan, C. Meza, and J. J. Negroni, "Energybalance control of PV cascaded multilevel grid-connected inverters under level-shifted and phase-shifted PWMs," *IEEE Trans. Ind. Electron*., vol. 60, no. 1, pp. 98–111, Jan. 2013.

[10]. L. Xi, G. Baoming, and P. Fang Zheng, "Minimizing dc capacitance requirement of cascadeded H-bridge multilevel inverters for photovoltaic systems by 3rd harmonic injection," in Proc. 27th Annu. *IEEE Appl. Power Electron. Conf. Expo. (APEC)*, 2012, pp. 240–245.

[11]. M. A. P. Oliveira and M. B. R. Correa, "Analysis of grid-tied single phase multilevel inverters powered by photovoltaic panels under partial shading conditions," in *Proc. 3rd IEEE Int. Symp. Power Electron. Distrib. Gener. Syst. (PEDG)*, 2012, pp. 483–486.

[12]. Z. Wei, C. Hyuntae, G. Konstantinou, M. Ciobotaru, and V. G. Agelidis, "Cascaded H-bridge multilevel converter for large-scale PV gridintegration with isolated dc–dc stage," in *Proc. 3rd IEEE Int. Symp. Power Electron. Distrib. Gener. Syst. (PEDG)*, 2012, pp. 849–856.

[13]. X. Bailu, S. Ke, M. Jun, F. Filho, and L. M. Tolbert, "Control of cascaded H-bridge multilevel inverter with individual MPPT for grid-connected photovoltaic generators," in *Proc. IEEE Energy Convers. Congr. Expo. (ECCE)*, 2012, pp. 3715–3721.

[14]. F. Wu, B. Sun, J. Duan, and K. Zhao, "On-line variable topology-type photovoltaic grid-connected inverter," *IEEE Trans. Ind. Electron*., vol. 62, no. 8, pp. 4814–4822, Aug. 2015.

[15]. Y. Liu, B. Ge, H. Abu-Rub, and F. Z. Peng, "An effective control method for three-phase quasi-Z-source cascaded multilevel inverter based grid-tie photovoltaic power system," *IEEE Trans. Ind. Electron*., vol. 61, no. 12, pp. 6794–6802, Dec. 2014.

[16]. D. Sun et al., "Modeling, impedance design, and efficiency analysis of quasi-Z-source module in cascaded multilevel photovoltaic power system," *IEEE Trans. Ind. Electron*., vol. 61, no. 11, pp. 6108–6117, Nov. 2014.

[17]. Y. Yu, G. Konstantinou, B. Hredzak, and V. G. Agelidis, "Operation of cascaded h-bridge multilevel converters for large-scale photovoltaic power plants under bridge failures," *IEEE Trans. Ind. Electron*., vol. 62, no. 11, pp. 7228–7236, Nov. 2015.

[18]. J. Yuncong, J. A. A. Qahouq, and T. A. Haskew, "Adaptive step size with adaptive-perturbation-frequency digital MPPT controller for a singlesensor photovoltaic solar system*," IEEE Trans. Power Electron*., vol. 28, no. 7, pp. 3195–3205, Jul. 2013.

[19]. E. S. Sreeraj, K. Chatterjee, and S. Bandyopadhyay, "One-cyclecontrolled single-stage single-phase voltage-sensorless grid-connected PV system," *IEEE Trans. Ind. Electron*., vol. 60, no. 3, pp. 1216–1224, Mar. 2013.

[20]. E. Dallago, D. G. Finarelli, U. P. Gianazza, A. L. Barnabei, and A. Liberale, "Theoretical and experimental analysis of an MPP detection algorithm employing a single-voltage sensor only and a noisy signal," *IEEE Trans. Power Electron*., vol. 28, no. 11, pp. 5088–5097, Nov. 2013.

[21]. E. Dallago, A. Liberale, D. Miotti, and G. Venchi, "Direct MPPT algorithm for PV sources with only voltage measurements," *IEEE Trans. Power Electron*., vol. 30, no. 12, pp. 6742–6750, Dec. 2015.

[22]. L. Yidan and W. Bin, "A novel d c voltage d etection technique in the CHB inverter-based STATCOM," *IEEE Trans. Power Del*., vol. 23, no. 3, pp. 1613–1619, Jul. 2008.

[23]. G. Farivar, V. G. Agelidis, and B. Hredzak, "A generalized capacitors voltage estimation scheme for multilevel converters," in *Proc. 16th Eur. Conf. Power Electron. Appl. (EPE)*, 2014, pp. 1–5.

[24]. J. de Leon Morales, M. F. Escalante, and M. T. Mata-Jimenez, "Observer for dc voltages in a cascaded H-bridge multilevel STATCOM," *IET Elect. Power Appl*., vol. 1, pp. 879–889, 2007.

[25]. M. C. Cavalcanti, G. M. S. Azevedo, B. A. Amaral, K. C. de Oliveira, F. A. S. Neves, and Z. D. Lins, "Efficiency evaluation in grid connected photovoltaic energy conversion systems," in *Proc. 36th IEEE Power Electron. Spec. Conf. (PESC)*, 2005, pp. 269–275.

[26]. G. Farivar, B. Hredzak, and V. G. Agelidis, "Decoupled control system for cascaded H-bridge multilevel converter based STATCOM*," IEEE Trans. Ind. Electron*., vol. 63, no. 1, pp. 322–331, Jan. 2016.

[27]. S. Kouro, P. Lezana, M. Angulo, and J. Rodriguez, "Multicarrier PWM with dc-link ripple feedforward compensation for multilevel inverters," *IEEE Trans. Power Electron*., vol. 23, no. 1, pp. 52–59, Jan. 2008.

[28]. G. Farivar, B. Hredzak, and V. G. Agelidis, "Reduced-capacitance thinfilm H-bridge multilevel STATCOM control utilizing an analytic filtering scheme," *IEEE Trans. Ind. Electron*., vol. 62, no. 10, pp. 6457–6468, Oct. 2015.

[29]. G. Farivar and B. Asaei, "A new approach for solar module temperature estimation using the simple diode model," *IEEE Trans. Energy Convers*., vol. 26, no. 4, pp. 1118–1126, Dec. 2011.

[30]. G. Farivar, B. Asaei, and S. Mehrnami, "An analytical solution for tracking photovoltaic module MPP," *IEEE J. Photovolt.*, vol. 3, no. 3, pp. 1053–1061, Jul. 2013.

Harsha Patle." A Novel Dc Voltage Detection Technique in Cascaded H-Bridge Multilevel Converter Based Photovoltaic System" International Refereed Journal of Engineering and Science (IRJES), vol. 07, no. 05, 2018, pp. 18–29.